AIAA JOURNAL
Vol. 36, No. 2, February 1998

Application of Method of Characteristics to Underexpanded, Freejet Flows with Vibrational Nonequilibrium

Jennifer L. Palmer* and Ronald K. Hanson†
Stanford University, Stanford, California 94305-3032

The method of characteristics (MOC) is employed computationally in the simulation of planar or axisymmetric, steady, supersonic flows in highly underexpanded freejets. The gas is assumed to be inviscid and nonreacting but may be vibrationally frozen, relaxing, or equilibrated. The ordinary-differential equations obtained by the MOC are integrated along the characteristics by a combined second-order, explicit–first-order, implicit method in regions of the flow with relatively rapid vibrational energy transfer (VET) and by a fully second-order, explicit method in regions with either slow or very rapid VET. Results from MOC simulations of flows with constant specific-heat ratios are verified by comparison with results obtained in previous MOC computations of expansion-fan flows and with empirically based correlations giving the size of the barrel-shock structure as a function of stagnation-to-ambient-pressure ratio. Comparisons are also made between MOC results for a vibrationally relaxing gas and results for vibrationally frozen and equilibrated gases, to verify the computational methods used to simulate flows with VET. The demonstrated capability for simulating underexpanded freejet flowfields represents a useful tool for predicting the results of experiments conducted in a small-scale shock-tunnel facility.

Nomenclature

a	= sound speed
C	= characteristic curve (any right- or left-running characteristic or streamline)
c	= specific heat
D	= nozzle throat diameter
e	= energy per unit mass
g	= degeneracy of an internal energy mode
h	= enthalpy per unit mass
M	= Mach number, total number of internal energy modes
N	= total number of points or species
P	= pressure
R	= gas constant per unit mass
r	= radial spatial dimension
T	= temperature
t	= time
V	= magnitude of velocity vector
$\boldsymbol{V}$	= velocity vector
X	= species mass fraction
x	= horizontal spatial dimension
y	= vertical spatial dimension
α	= angle of a Mach line with respect to the x axis
β	= angle between consecutive right-running characteristics at the origin of an expansion fan
γ	= ratio of specific heats
δ	= coefficient allowing generalized treatment of two-dimensional flows by the method of characteristics
ζ	= source term for vibrational energy
Θ	= characteristic temperature
θ	= flow angle with respect to the x axis
ρ	= density
τ	= characteristic time for relaxation
χ	= species mole fraction
Ψ	= relative departure of vibrational energy of lowest energy mode from equilibrium

Subscripts

a	= ambient condition
atom	= atomic species
disk	= Mach disk
froz	= vibrationally frozen
i	= initial-value line
low	= lowest energy
m	= index of internal energy mode
n, n'	= index of species
n–n'	= VET from species n in collisions with molecules of species n'
p	= constant pressure
rot	= rotational mode
s	= stagnation condition
trip	= triple point
vib	= vibrational mode or vibrationally active species
0	= streamline
+	= left-running characteristic
−	= right-running characteristic

Superscripts

VET	= vibrational energy transfer
V–T	= vibrational–translational
V–V	= vibrational–vibrational
*	= local vibrational equilibrium or triple-point location that allows satisfaction of downstream boundary condition

Introduction

THE use of the method of characteristics (MOC), a powerful and reliable technique for the computation of supersonic flowfields, is well documented.[1,2] In the present work, it has been applied to the simulation of several steady, inviscid, supersonic flowfields, with the ultimate goal of computing highly underexpanded freejets with vibrational relaxation. The primary motivation for this undertaking was to provide relatively simple and fast analyses of quasi-steady freejets created in a reflection-type shock-tunnel facility used for the development of diagnostic techniques.[3] More generally, the resulting collection of numerical models may be used to study a variety of planar and axisymmetric flows with important practical applications.

Figure 1 illustrates the flowfields that have been computed with the MOC, including supersonic nozzle flows, moderately underexpanded freejets, and highly underexpanded freejets. In each case, the flow downstream of the nozzle throat is calculable. Any contours

Received Nov. 26, 1996; revision received Aug. 14, 1997; accepted for publication Sept. 16, 1997.

*Graduate Research Assistant, High Temperature Gasdynamics Laboratory, Department of Mechanical Engineering; currently Senior Mechanical Engineer, Lockheed Martin Missiles and Space, Orgn. E5-40, Building 157, 1111 Lockheed Martin Way, Sunnyvale, CA 94089. Student Member AIAA.

†Chairman, Department of Mechanical Engineering, Building 520, Room 520E. Fellow AIAA.

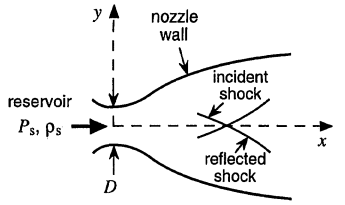

a) Supersonic nozzle with oblique shock waves

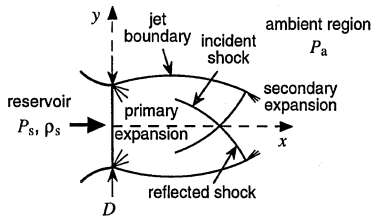

b) Moderately underexpanded freejet ($2 \lesssim P_s/P_a \lesssim 4$)

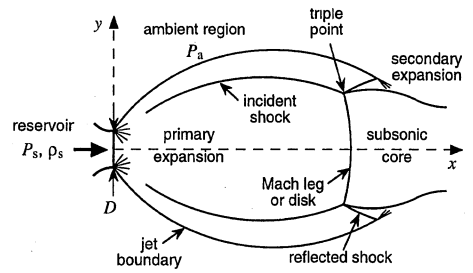

c) Highly underexpanded freejet ($P_s/P_a \gtrsim 4$)

Fig. 1 Examples of flowfields calculable with the MOC.

may be used for the nozzle walls, although the current discussion is restricted to flows with an axis of symmetry and, furthermore, to those for which conditions at the nozzle throat are known. Another restriction is that the flow must remain supersonic throughout the region of interest, which does not exclude the appearance of oblique shocks or even the strong shock labeled the Mach leg or disk in Fig. 1c, though a one-dimensional solution must be patched into the model to treat the subsonic core downstream of it. Zucrow and Hoffman[2] provide a procedure for the calculation of supersonic nozzle flowfields without discrete shocks. It has been modified to include shocks by methods incorporated in previous MOC calculations and serves as the basis for the development of a freejet simulation.

Pack[4] performed one of the earliest calculations of a freejet flowfield by the MOC, using planar geometry and a low pressure ratio to minimize the necessary calculations, although incident and reflected shocks were included. The flow in a high-pressure-ratio jet, including the incident shock, has commonly been calculated upstream of the Mach disk by the MOC.[5–8] Extension of the calculation farther downstream was attempted by several authors,[9,10] before the problem of properly placing the Mach disk was solved by Abbett,[11] with a strategy that is based on physical reasoning and yields predictions that agree with experimental results.[12]

Computational techniques other than the MOC have also been used in freejet simulations.[13–18] Typically, the MOC has advantages over other methods in accuracy and in the treatment of shocks and flow boundaries as discrete discontinuities, although MOC routines are often considered logically more complex and computationally more intensive.[2] However, the speed and memory capabilities of modern work stations have reduced the long computational times traditionally associated with the MOC, and shock- and boundary-capturing strategies have been successfully implemented in other types of calculations.[13,14,19]

The MOC has been applied to a variety of basic gas-dynamic flows with nonequilibrium, including flow over a wedge, cone, or blunt body[20–23] and around a sharp corner.[24,25] These calculations include some of the basic features of the freejet flowfield and demonstrate the approaches to be taken. Simulations of relaxing flows in supersonic nozzles have also been performed,[26–29] as well as inverse calculations in which a nozzle contour yielding a desired outlet condition is determined.[26,27] The relaxation processes involve the rotational,[30] vibrational,[21–23,25–27] chemical,[20,22–29] and/or ionizational[23,25] states of the gas, usually independently and sometimes interchangeably. Typically, the frozen and equilibrium conditions of the flow are investigated as bounds of the full nonequilibrium solution. The effects of particles in chemically nonreacting[31,32] and reacting[33] flows have also been studied.

Landau–Teller theory, describing the evolution of a Boltzmann distribution of harmonic oscillators toward equilibrium with the translational–rotational state of the gas, has been found to accurately model vibrational energy transfer (VET) in most compressive flows.[34,35] It predicts that vibrational relaxation occurs with a characteristic time that is inversely proportional to pressure and, otherwise, purely a function of molecular parameters and translational temperature and that the rate of energy transfer is proportional to the deviation of the vibrational energy from its value at the local equilibrium condition.[35] Therefore, vibrational deexcitation should occur at the same rate as excitation, under similar conditions. However, at very high temperatures, excitation rates in shock-tube flows have been observed to deviate slightly from the linear theory,[36–38] and measurements of lower-level vibrational population distributions in supersonic nozzle flows have indicated the presence of rapid relaxation mechanisms not predicted by the Landau–Teller equation.[39–42] Rates 5–1000 times higher than those measured in excitation studies may be necessary to match the observed relaxation times in flows undergoing vibrational de-excitation,[43] although this is not always the case.[44–46]

The discrepancies in observations of compressive and expansive flows were resolved with a more accurate theory of VET that includes the effects of anharmonicity and state-dependent vibrational–translational (V–T) and vibrational–vibrational (V–V) energy-transfer rates.[47,48] Very rapid vibrational relaxation, as measured by changes in the populations of low-lying vibrational levels of the gas species, is found to result from rapid upper-level V–T transfer and from pumping of lower-level population to higher levels by V–V processes. The resulting highly non-Boltzmann vibrational distributions, i.e., population inversions, have been observed experimentally[49,50] and in simulations of rapidly expanding gases.[49–53] The Landau–Teller equation is found to be a limiting case of the anharmonic-oscillator theory, accurate for a relaxing gas without significant upper-level populations initially present.

Several difficulties arise in any attempt to use the anharmonic-oscillator model in flowfield calculations. Foremost among these is the lack of adequate rate data describing level-dependent V–T and V–V processes in mixtures of gases, e.g., air.[49,52,54] Although theoretical models of the transition processes have been developed, their accuracy depends on calibration with scarce experimental data.[52,53] Generally, only qualitatively correct results for vibrational energy distributions and overall relaxation behavior are obtainable in simulations of expanding flows. Another concern lies in the very long computation times that would be expected in a multidimensional flowfield calculation including a complete analysis of the vibrational state of the gas.[46] Consequently, the Landau–Teller model is often used in simulations of supersonic nozzle flowfields.[27,55] An energy-averaged definition of vibrational temperature may, however, be incorporated to partially account for the effects of non-Boltzmann population distributions.[56]

In the present work, an extended linear theory including nonresonant V–V transfer is employed,[57] permitting a qualitative description of vibrational relaxation in nozzle and freejet flowfields. Energy-transfer rates, generally measured in shock-tube studies, may be varied, i.e., multiplied by a factor of 1–1000, to examine the probable effects of anharmonicity and rapid upper-level V–T processes on the vibrational temperature characterizing the lowest vibrational levels of each gas component. These results are likely to be as useful in the prediction of bulk nonequilibrium effects as those from a full analysis because of the uncertainties in the rate data.

Formulation

The equations describing the conservation of mass, momentum, and energy for a steady, inviscid flow in two dimensions, i.e., x, an axial coordinate, and y (or r), a transverse (or radial) coordinate, may be written as

$$\nabla \cdot (\rho V) = 0 \tag{1}$$

$$\rho\frac{\mathrm{D}V}{\mathrm{D}t}+\nabla P=0 \tag{2}$$

and

$$\rho\frac{\mathrm{D}}{\mathrm{D}t}\left(h+\frac{1}{2}V^2\right)=0 \tag{3}$$

The system of equations is completed with the perfect-gas equation of state and a constitutive relation

$$P=\rho RT \tag{4}$$

and

$$h=c_{p,\mathrm{froz}}T+e_{\mathrm{vib}} \tag{5}$$

respectively, where $c_{p,\mathrm{froz}}$ is the specific heat under vibrationally frozen conditions, defined by

$$\frac{c_{p,\mathrm{froz}}}{R}=\frac{5}{2}+\sum_{n=1}^{N_{\mathrm{vib}}}\chi_n\sum_{m=1}^{M_{\mathrm{rot},n}}\frac{g_{\mathrm{rot},n,m}}{2} \tag{6}$$

The vibrational energy of the gas mixture is given by

$$e_{\mathrm{vib}}=\sum_{n=1}^{N_{\mathrm{vib}}}X_n e_{\mathrm{vib},n} \tag{7}$$

where the vibrational energy of species n is

$$e_{\mathrm{vib},n}=\sum_{m=1}^{M_{\mathrm{vib},n}}g_{\mathrm{vib},n,m}e_{\mathrm{vib},n,m} \tag{8}$$

and

$$e_{\mathrm{vib},n,m}=R_n\Theta_{\mathrm{vib},n,m}\Big/\exp\left\{\frac{\Theta_{\mathrm{vib},n,m}}{T_{\mathrm{vib},n}}\right\}-1 \tag{9}$$

Each molecular species is assumed to maintain internal equilibrium among its vibrational modes; thus, the Boltzmann population distribution of each mode is characterized by the same vibrational temperature $T_{\mathrm{vib},n}$.

A modified version of the Landau–Teller model, similar to that derived by Taylor et al.,[57] is used to represent vibrational relaxation in a gas mixture with N_{atom} atomic and N_{vib} vibrationally active species,

$$\frac{\mathrm{D}e_{\mathrm{vib},n,m}}{\mathrm{D}t}=\zeta_{n,m}$$

$$n=1,2,\ldots,N_{\mathrm{vib}},\qquad m=1,2,\ldots,M_{\mathrm{vib},n} \tag{10}$$

where

$$\zeta_{n,m}=\frac{c_{\mathrm{vib},n,m}(T_{\mathrm{vib},n})}{c_{\mathrm{vib},n,m_{\mathrm{low}}}(T_{\mathrm{vib},n})}\zeta_{n,m_{\mathrm{low}}} \tag{11}$$

$$\frac{c_{\mathrm{vib},n,m}(T)}{R_n}=\left(\frac{\Theta_{\mathrm{vib},n,m}}{T}\right)^2\exp\left\{\frac{\Theta_{\mathrm{vib},n,m}}{T}\right\}\Big/\left(\exp\left\{\frac{\Theta_{\mathrm{vib},n,m}}{T}\right\}-1\right)^2 \tag{12}$$

$$\frac{\zeta_{n,m_{\mathrm{low}}}}{e^*_{\mathrm{vib},n,m_{\mathrm{low}}}}=\sum_{n'=1}^{N_{\mathrm{atom}}+N_{\mathrm{vib}}}\frac{\chi_{n'}}{\tau^{\mathrm{V-T}}_{n-n'}}\Psi_n+\sum_{\substack{n'=1,\\ n'\neq n}}^{N_{\mathrm{vib}}}\frac{\chi_{n'}}{\tau^{\mathrm{V-V}}_{n-n'}}\times\left[\Psi_n(1-\Psi_{n'})\frac{1-\exp\{-\Theta_{\mathrm{vib},n,m_{\mathrm{low}}}/T\}}{1-\exp\{-\Theta_{\mathrm{vib},n',m_{\mathrm{low}}}/T\}}-\Psi_{n'}(1-\Psi_n)\right] \tag{13}$$

and

$$\Psi_n=\frac{e^*_{\mathrm{vib},n,m_{\mathrm{low}}}-e_{\mathrm{vib},n,m_{\mathrm{low}}}}{e^*_{\mathrm{vib},n,m_{\mathrm{low}}}} \tag{14}$$

Only single-quantum VET is allowed and the series approximation is used to account for the vibrational relaxation of polyatomic species.[58] Therefore, it is assumed that, if a molecule has multiple vibrational modes, VET to and from that species occurs only through its lowest-energy mode m_{low}. Rapid internal redistribution and resonant V–V transfer in collisions with other molecules of the same species are assumed to effectively maintain Boltzmann distributions within each vibrational mode and between all modes of a single species. The characteristic times for V–T and V–V relaxation of species n in collisions with species n', $\tau^{\mathrm{V-T}}_{n-n'}$ and $\tau^{\mathrm{V-V}}_{n-n'}$, respectively, are functions of the local translational–rotational temperature and the gas pressure that refer to total VET times for all modes of the species[58,59] and must be obtained from experimental data.[3] The present numerical implementation of Eqs. (10–14) has been verified by comparing results obtained from a simulation of the flow behind a planar shock with the experimental data provided by Taylor et al.[57]

Recasting the equations in characteristic form in a manner similar to that used for constant-γ flows[2] yields three equations describing a family of streamlines (C_0) and two families of Mach lines (C_+ and C_-), all of which are known as characteristics, that is

$$\left(\frac{\mathrm{d}y}{\mathrm{d}x}\right)_0=\tan\theta \tag{15}$$

defining streamlines and

$$\left(\frac{\mathrm{d}y}{\mathrm{d}x}\right)_\pm=\tan(\theta\pm\alpha) \tag{16}$$

defining Mach lines, as well as $2+N_{\mathrm{vib}}$ ordinary-differential equations (ODEs) that apply along the streamlines and a single ODE that applies along each Mach line,

$$\rho V\,\mathrm{d}V_0+\mathrm{d}P_0=0 \tag{17}$$

$$\mathrm{d}P_0-a^2\,\mathrm{d}\rho_0+(\gamma-1)\rho\sum_{n=1}^{N_{\mathrm{vib}}}X_n\sum_{m=1}^{M_{\mathrm{vib},n}}\mathrm{d}(e_{\mathrm{vib},n,m})_0=0 \tag{18}$$

and

$$\mathrm{d}\left(e_{\mathrm{vib},n,m_{\mathrm{low}}}\right)_0-\frac{\zeta_{n,m_{\mathrm{low}}}}{V\cos\theta}\,\mathrm{d}x_0=0,\qquad n=1,2,\ldots,N_{\mathrm{vib}} \tag{19}$$

along streamlines and

$$\frac{\sqrt{M^2-1}}{\rho V^2}\,\mathrm{d}P_\pm\pm\mathrm{d}\theta_\pm+\left[\frac{\delta\sin\theta}{yM}+\frac{(\gamma-1)}{V^2a}\sum_{n=1}^{N_{\mathrm{vib}}}X_n\sum_{m=1}^{M_{\mathrm{vib},n}}\zeta_{n,m}\right]\frac{\mathrm{d}x_\pm}{\cos(\theta\pm\alpha)}=0 \tag{20}$$

along Mach lines. The ratio of specific heats and all quantities dependent on it have their frozen values, i.e., $\gamma=c_{p,\mathrm{froz}}/(c_{p,\mathrm{froz}}-R)$, $a=\sqrt{(\gamma P/\rho)}$, $M=V/a$, and $\alpha=\sin^{-1}(1/M)$, as is usually the case in MOC simulations of flows with nonequilibrium.[30] The upper parts of the $\pm$ signs used in Eqs. (16) and (20) apply to the C_+ family of characteristics, known as left-running characteristics (LRCs), whereas the lower parts apply to the C_- family of characteristics, known as right-running characteristics (RRCs). The parameter δ, necessary to account for geometrical differences, is 0 for planar flows and 1 for axisymmetric flows. An arbitrary point in the flowfield, through which a characteristic of each of the three families passes, is shown in Fig. 2.

Figure 3 shows two methods by which the flow conditions may be determined at an interior point in the flow. In each case, the solid lines are those that are followed by the computation, whereas the dashed lines indicate those that are not tracked and, therefore, are used temporarily and then discarded. In Fig. 3a, an LRC and an RRC intersect at the location of a new data point, and the streamline is rearwardly projected to a line drawn between the two original points, where linear interpolation is used to determine the properties. To find the location of the new point and its properties, Eqs. (17–20) are integrated along the curves defined by Eqs. (15) and (16). Alternatively, as shown in Fig. 3b, C_- and C_0 families may be tracked, whereas the LRCs are rearwardly projected. In each case, as additional downstream points are determined, a web-like pattern, called a solution network, is formed by the permanent characteristics. It has been argued that in chemically relaxing flows, interpolation for the varying chemical composition of the gas along streamlines may result in significant error being propagated downstream.[2,28] For such a problem, the grid type shown in Fig. 3b would seem to be the natural choice. However, for vibrationally relaxing flows, interpolation for

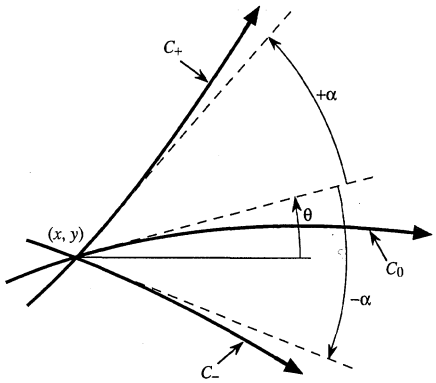

Fig. 2 Characteristics C_+, C_-, and C_0 at point (x,y) in the flowfield. The streamline (C_0) lies at an angle θ with respect to the positive x axis. LRCs (C_+) and RRCs (C_-) are known as Mach lines and are inclined at $+\alpha$ and $-\alpha$, respectively, with respect to the streamlines in the streamwise direction.

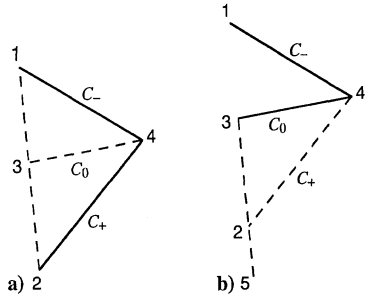

Fig. 3 Two strategies for tracking characteristics through the flowfield and determining the solution at a new point: a) new data point, i.e., 4, is formed at the intersection of C_- and C_+, and C_0 passing through that point is projected back to the line between the original data points, i.e., 1 and 2; and b) new data point, i.e., 4, is formed at the intersection of C_- and C_0, and C_+ passing through that point is projected back to the line between two of the original data points, i.e., 3 and 5.

the vibrational energy is unlikely to lead to excessive error, allowing the method shown in Fig. 3a to be used throughout the present work.[30]

Numerical Implementation

The strategy for the numerical simulation of a steady, two-dimensional, supersonic flow was developed by Zucrow and Hoffman,[2] who employ a master logic program that calls various subroutines, termed unit processes, to solve an appropriate set of difference equations describing the intersection of an RRC and an LRC, i.e., an interior point, the intersection of two characteristics of the same family, i.e., a shock point, or the intersection of a characteristic and a flow boundary, e.g., an RRC and an axis of symmetry, in the case of an axis point. The logic program provided by Zucrow and Hoffman[2] may be used to compute the flow in a diverging nozzle without shocks, and a modified version of it has been used for nozzle flows containing shocks. Computer codes that simulate underexpanded freejets with Mach diamonds and disks have also been developed in the computer language Fortran77 (Ref. 3).

The modified Euler predictor–corrector method with iteration, which Zucrow and Hoffman[2] use to numerically integrate the coupled set of ODEs describing a flow with constant γ, is stable and yields small absolute errors for reasonably small spatial-step sizes, i.e., initially on the order of $\frac{1}{10}$th of the characteristic spatial dimension D. Finite difference equations are obtained for computational use of the MOC by substituting $\Delta()_\pm$ or $\Delta()_0$, the difference in a flow variable between two adjacent points on $C_\pm$ or C_0, respectively, for $\mathrm{d}()_\pm$ or $\mathrm{d}()_0$ in the characteristic and compatibility equations. Averaged values of the flow properties between points along the characteristics are used to evaluate the coefficients, making the corrector, and thus the entire solution, of second-order accuracy. The solution begins with a prediction based on an explicit, first-order Euler scheme, after which corrected values of the properties of the new point (and the location of the rearwardly projected point) are determined from the finite difference equations. The corrector is applied a fixed number of times or until the specified convergence tolerance for each variable is met in successive iterations.

For isentropic flows, the subroutines provided by Zucrow and Hoffman[2] for interior, axis, jet-boundary, and nozzle-wall points may be used directly. The inclusion of equations describing the relaxation of the vibrational or chemical state of the gas, however, results in a set of ODEs that becomes stiff in a mathematical sense when the characteristic time required to reach local equilibrium, i.e., τ, becomes small compared with the fluid-mechanical residence time, i.e., $D\sqrt{(\rho/P)}$ (Refs. 2 and 60). An unreasonably small spatial-step size, hundreds or thousands of times less than normal, may be required to maintain the numerical stability of the solution, if an explicit numerical integration scheme is used. The number of computations required for the simulation of a multidimensional flowfield with active relaxation processes may, however, be greatly reduced by the use of an implicit scheme, which allows a step size on the order of the physical dimensions of the flow of interest, regardless of the rates of energy transfer or reaction.[60]

A combined implicit–explicit integration scheme has been implemented in the unit processes used to solve the equations governing the flow of a vibrationally relaxing gas mixture to increase the efficiency of the solution procedure, while maintaining its stability at reasonably large spatial-step sizes.[28,60] The ODEs, other than Eq. (19), are converted to difference equations by the method already described. The relaxation equations are converted to difference equations by the same method, if the quantity $\Delta x_0/(V\cos\theta)$, i.e., the local temporal-step size, is less than the smallest effective VET time constant, $\tau_{\min}^{\mathrm{VET}}\{=[(e^*_{\mathrm{vib},n,m_{\mathrm{low}}} - e_{\mathrm{vib},n,m_{\mathrm{low}}})/\zeta_{n,m_{\mathrm{low}}}]_{\min}\}$, or by replacing the differentials with the first-order terms in Taylor series expansions about the downstream point,[60] if $\Delta x_0/(V\cos\theta) \geq \tau_{\min}^{\mathrm{VET}}$. As before, averaged values of the flow properties are used to evaluate the coefficients in the equations, except for Eq. (19), when $\Delta x_0/(V\cos\theta) \geq \tau_{\min}^{\mathrm{VET}}$, in which case the properties at the new point are used to determine the quantity $\zeta_{n,m_{\mathrm{low}}}/(V\cos\theta)$. If $\Delta x_0/(V\cos\theta) \geq 5\times\tau_{\max}^{\mathrm{VET}}\{=[(e^*_{\mathrm{vib},n,m_{\mathrm{low}}} - (e_{\mathrm{vib},n,m_{\mathrm{low}}})/\zeta_{n,m_{\mathrm{low}}}]_{\max}$, the largest VET time constant}, Eq. (19) is abandoned, and the vibrational energies are simply assigned their local equilibrium values, given by Eq. (9) with $T_{\mathrm{vib},n} = T$. Thus, a purely second-order, explicit integration method is used in regions of the flow with relatively slow VET and in regions with very rapid VET. A combined second-order, explicit–first-order, implicit method is used in regions with moderately rapid VET. As Tyson[60] observed, mild instability persists when the temporal-step size is much larger than the relaxation time constant because of the use of explicit integration for the energy equation, or, in the present case, Eq. (18), which is derived from the energy equation. Stability problems in the freejet simulations occur primarily near the nozzle lip, where large vibrational-energy gradients exist along the Mach lines as a result of the frozen vibrational state at the nozzle lip and the near-equilibrium condition at neighboring points.

Points on shock waves are approached in a manner similar to that used for other points, although they require the additional use of the oblique-shock relations,[1] which may be employed directly, as the flow across the shock is vibrationally frozen, and an equation describing the shape of the shock, similar to those given for the characteristics by Eqs. (15) and (16). An iterative, multidimensional Newton–Raphson technique[61] is used to solve the coupled difference equations, because of their greater number and complexity than for points not involving shocks. Initial guesses for the flow properties are obtained by projecting characteristics, shocks, and flow boundaries along straight-line paths to their intersections, as is done by the predictor of the modified Euler method. The required derivatives of the functions with respect to each variable are obtained numerically. The iterations continue until the convergence criteria are satisfied or until a specified number are completed.

Solution Procedure

Several strategies may be employed to create an initial-value (IV) line from which the MOC calculation for a vibrationally relaxing gas can proceed. Caution must be exercised, however, because an arbitrarily chosen value for the vibrational energy of the gas may result in physically unrealistic flow adjustments downstream of the nozzle

exit.[29] The simplest method of constructing a realistic IV line relies on the assumption that the flow is uniform, slightly supersonic, and in vibrational equilibrium at the nozzle exit. An IV line having N_i evenly spaced points may thus be created, with $M = M_i$, $\theta = 0$, and the other flow properties determined from the stagnation conditions by use of the isentropic-flow relations.[1] Alternatively, equations describing the one-dimensional flow of a vibrationally relaxing gas may be integrated from the stagnation region, where equilibrium is assumed to exist, to a position just past the nozzle throat. This method is complicated by the fact that the mass-flow rate through the nozzle is not known a priori and because the equations are singular at the throat, if the calculation is based on a prescribed variation of the area of the nozzle with distance. Although these difficulties may be surmounted, the resulting computations are usually lengthy and represent a level of detail frequently unnecessary for accurate simulation of the flowfield downstream. Regardless of which assumption is made about the vibrational state of the gas in the converging nozzle, the two-dimensional perturbation analysis of the nozzle flowfield by Kleigel and Quan[62] may be used to include the effect of the nozzle-wall curvature by employing an average expansion coefficient, if desired.

The intersection of the RRC originating at the IV point just above the axis with the LRC originating at the point on the axis forms the first new data point in the flowfield. A solution that satisfies the appropriate boundary conditions, i.e., no flow or property gradients normal to the axis, is then determined at the point where the RRC intersects the axis, and the first point on a new LRC is created. The RRC originating at the next point on the IV line is extended through its intersections with the LRC originating at the IV point nearest the axis, the LRC originating at the IV point on the axis, and the LRC created by the reflection of the previous RRC. It, too, is terminated at the axis and an LRC, representing its reflection, is established. This process is repeated for each successively higher point on the IV line, until the solution in the area of the flow known as the IV region is completed.

The computation is now specialized to the case of a freejet, and the first point in the expansion fan originating at the nozzle lip is obtained by projecting an RRC from it with a specified angular spacing from the last RRC in the IV region. The conditions at the nozzle lip are determined from the Prandtl–Meyer relation,[1] and the RRC is extended to the axis in the same manner as were the previous RRCs. The creation of RRCs at the nozzle lip continues until the pressure falls below that in the ambient region, then the flow properties at the nozzle lip are computed from the isentropic-flow relations,[1] with $P = P_a$, and a final RRC is computed, completing the simulation of the primary expansion fan. Each RRC is separated from the preceding one by an angle β, with the exception of the first and second RRCs in the fan, which are spaced by $\beta/2$ to maintain a fairly regular grid downstream, and the final RRC, which is spaced by whatever angle ($\leq\beta$) is required to satisfy the boundary condition.

The simulation continues with the reflection of the LRC nearest the nozzle lip from the jet boundary, which requires the solution of the difference forms of the characteristic and compatibility equations describing the LRC and the streamline along the jet boundary with the constant-pressure boundary condition. An attempt is then made to extend the RRC created at the reflection point to the axis in the manner described earlier. The compression introduced at the jet boundary, however, causes the RRC to intersect the previous one before it reaches the axis, at which point a right-running incident shock is inserted, and the intersecting RRCs are terminated. The solution at the first shock point is determined by solving the characteristic and compatibility equations for the two RRCs along with those for an LRC and a streamline rearwardly projected from the shock point and the shock-jump relations.[1] The next LRC in the primary expansion fan is then reflected from the jet boundary, and the process is repeated until the resulting RRC reaches the shock. LRCs are extended through the shock, creating new points on it, to their intersections with the current RRC. When the RRC intersects the shock wave, it is terminated and an RRC is created at the jet boundary. RRCs located upstream of the shock may also intersect it, at which point they are terminated as well.

For small pressure ratios, i.e., $2 \lesssim P_s/P_a \lesssim 4$, the process of creating RRCs at the jet boundary and extending them to the shock continues, until the incident shock reaches the axis, forming a reflected shock at an angle determined by the condition requiring no flow normal to the axis downstream of the reflection point. The intersection of the reflected shock with the RRC just downstream of the last point on the incident shock is then determined, and the RRC is extended to the axis, where an LRC is formed. RRCs are created at the jet boundary and extended to the axis, through the reflected shock, until it reaches the jet boundary and is reflected as an expansion. RRCs are then created at the origin of the secondary expansion fan with the same specified angular separation β, extended toward the axis, and terminated when the flow becomes subsonic.[3]

The procedure for calculating the flow in a jet with a high value of $P_s/P_a (\gtrsim 4)$ is identical to that for a moderately underexpanded jet, up to the point at which an attempt is made to allow the incident shock to reflect from the axis. In the Mach-disk regime, regular reflection is impossible; a Mach-type reflection occurs instead, creating the barrel-shock structure and subsonic core shown in Fig. 1c. The axial location of the triple point x_{trip} is initially guessed and then used as the variable parameter in an iterative procedure based on the requirement that the quasi-one-dimensional flow in the core become critical at a throat-like area constriction,[11] whereas its radial position r_{trip} is given by that of the incident shock at x_{trip}. The MOC calculation proceeds as described for a low-pressure-ratio jet, until the incident shock extends past x_{trip}. The flow properties and shock angle at x_{trip} are found by linear interpolation between consecutive points, and a triple-shock point is inserted. The initial angles of the reflected shock, Mach disk, and core boundary are determined by the condition that no flow or pressure gradient exist across the slip line. Based on the position and slope of the Mach disk at the triple point and the requirement that it lie normal to the flow at the axis, a parabolic curve is introduced to represent the Mach disk.

The calculation continues in a manner similar to that described earlier for the propagation of a reflected shock, with the axis replaced by the boundary of the core, the properties of which evolve with each new point. When the reflected shock reaches the jet boundary, it is reflected as an expansion fan in which RRCs are created, as before, and extended to the core boundary. The computation of RRCs in the secondary expansion fan continues until the core flow either reaches a minimum area or becomes critical. If the value of x_{trip} is too small, the flow stagnates, reaching a minimum area without becoming critical; whereas, if x_{trip} is too large, it becomes critical before reaching a throat-like section. The desired value of x_{trip}, called x^*_{trip}, is that yielding critical core flow at a throat-like section. However, because x^*_{trip} is a saddle point, the downstream boundary condition is never satisfied exactly, and a value of x_{trip} arbitrarily close to x^*_{trip} is obtained.[11]

The grid structure yielded by the procedures described earlier for tracking characteristics through the various regions of the flow may be examined in Fig. 4, which shows the RRCs, LRCs, and

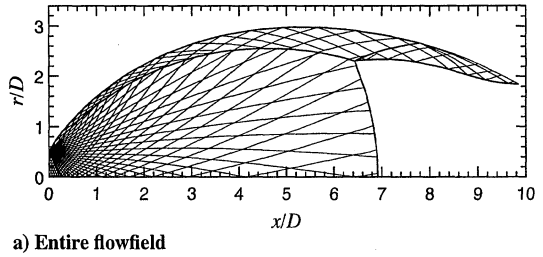

a) Entire flowfield

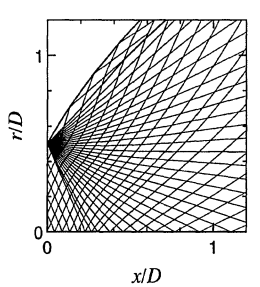

b) Region just downstream of the nozzle throat

Fig. 4 RRCs, LRCs, and primary features of a freejet with $\gamma = \frac{7}{5}$ and $P_s/P_a = 100$, computed with $\beta = 4$ deg from a uniform IV line with $M_i = 1.01$ and $N_i = 6$.

primary jet features obtained from an MOC calculation of a freejet of vibrationally frozen gas with $\gamma = \frac{7}{5}$ and $P_s/P_a = 100$, issuing from a sonic, axisymmetric nozzle throat with radially uniform flow properties. The simulation was performed with values of M_i, N_i, and β yielding a grid approximately four times coarser than would ordinarily be used, to allow the characteristics to be clearly seen.

Results

The validity of the MOC simulation for vibrationally frozen flows may be tested by comparison of the computed Mach number along the axis of an axisymmetric expansion fan with a correlation that is based on a fit of flow data calculated with the MOC.[63] Figure 5 shows comparisons between the correlation and the current MOC computations with several values of β, for three values of γ, i.e., $\frac{9}{7}$, $\frac{7}{5}$, and $\frac{5}{3}$. Ashkenas and Sherman[63] state that the formula accurately represents the flow from approximately the same lower limits of M for the various values of γ as are observed here. Departure of the MOC results from the correlation curves at large values of M occurs because of the increasingly large spacing of characteristics at large x/D. A decrease in β (or, secondarily, an increase in N_i) extends the range over which the MOC results match the correlation. Similarly good agreement is observed between the MOC results and a correlation for the radial variation of the flow properties in axisymmetric expansions.[63]

The computed values of x^*_{trip} and x_{disk} may be compared with empirical correlations for the axial distance from the nozzle exit to the Mach disk as a function of P_s/P_a, γ, and nozzle exit conditions. The correlations provide not only a simple check of the MOC results, but also the initial guess for x_{trip} needed to begin the simulation. Ashkenas and Sherman[63] present an experimentally based formula applicable to a freejet issuing from a sonic, axisymmetric nozzle: $x_{disk}/D = 0.67\sqrt{(P_s/P_a)}$, for $15 \leq P_s/P_a \leq 17{,}000$. The value of γ has no influence on x_{disk}, according to this expression and a similar one derived by Crist et al.[64] for pressure ratios as high as 3×10^5. Another empirical correlation, derived by Lewis and Carlson,[65] yields a similar relation when applied to a jet issuing from a sonic nozzle, the only difference being an extra multiplicative term, equal to 0.85 for $\gamma = 1.22$, 0.89 for $\gamma = 1.4$, and 0.93 for $\gamma = 1.67$. Ashkenas and Sherman[63] also give an estimate of the radius of the Mach disk, i.e., $r_{trip}/x_{disk} = 0.21$ and 0.24 at $P_s/P_a = 20$ and 1000, respectively, for $\gamma = \frac{7}{5}$, which may be compared directly with the value obtained by the MOC, i.e., r^*_{trip}.

In Fig. 6, the results of MOC simulations of freejets with $\gamma = \frac{5}{3}$, $\frac{7}{5}$, and $\frac{9}{7}$, performed with various values of β (<1 deg) from IV lines with $M_i = 1.001$ and N_i (≈ 25), are compared with the correlations for x_{disk}/D and r_{trip}/D (assuming a linear variation of r_{trip}/x_{disk} with P_s/P_a). The values of x^*_{trip}/D and x_{disk}/D computed by the MOC show no significant dependence on γ and indicate that the assumption of a parabolic shape for the Mach disk results in x_{disk}/D being only slightly, i.e., <13%, larger than x^*_{trip}/D over the ranges of γ and P_s/P_a considered. Excellent agreement is observed between the MOC results and the correlations for x_{disk}/D, which yield very similar results, as expected.

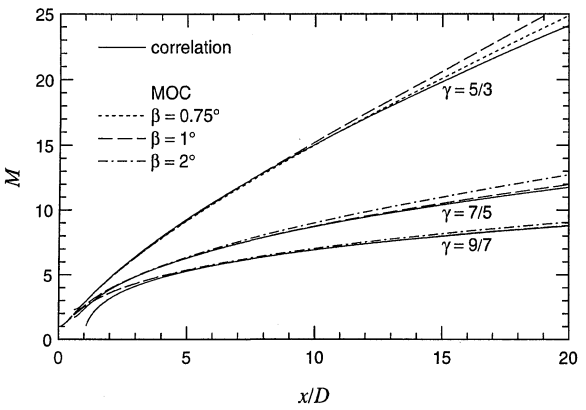

Fig. 5 Comparison of MOC results with a correlation given by Ashkenas and Sherman[63] for the variation of the Mach number along the centerline of an axisymmetric jet, i.e., $r = 0$.

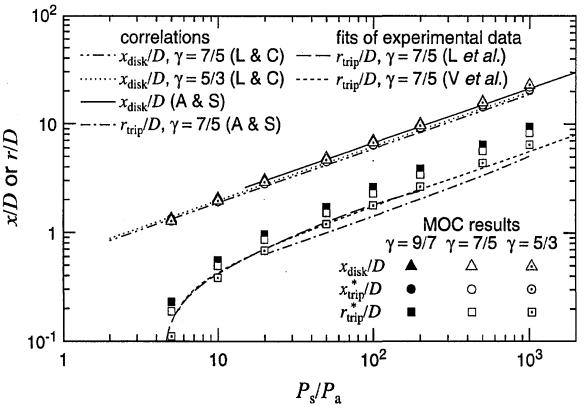

Fig. 6 MOC predictions of x^*_{trip}/D, r^*_{trip}/D, and x_{disk}/D as functions of P_s/P_a in freejets and the variations of x_{trip}/D and r_{trip}/D with P_s/P_a described by two correlations[63,65] and by polynomial fits of data[5,66] for r_{trip}/D.

Figure 6 also indicates that the computed value of r^*_{trip}/D at a given pressure ratio increases with decreasing γ, as Crist et al.[64] observed experimentally. For $P_s/P_a \geq 10$, values of r^*_{trip}/D for freejets with $\gamma = \frac{5}{3}$ and $\frac{9}{7}$ are consistently found to be ~20% less than and ~10% greater than, respectively, the corresponding value for a freejet with $\gamma = \frac{7}{5}$. At the lowest pressure ratio considered, i.e., $P_s/P_a = 5$, the relative differences are −40% and +20% for $\gamma = \frac{5}{3}$ and $\frac{9}{7}$, respectively. This observation suggests that the pressure ratio at which the transition from the Mach-diamond to the Mach-disk regime occurs increases with increasing γ, as the triple point has nearly reached the axis of the jet with $\gamma = \frac{5}{3}$. The general trend predicted for the radius of the Mach disk, i.e., that r_{trip}/x_{disk} increases with increasing P_s/P_a, is also displayed by the MOC results shown in Fig. 6; however, the value of r^*_{trip}/D (or r^*_{trip}/x_{disk}) for $\gamma = \frac{7}{5}$ is underestimated by 30–40%. Better agreement is observed between the MOC results and fourth-order polynomial fits of experimental data for r_{trip}/D as a function of P_s/P_a (Refs. 5 and 66). The discrepancies between the experimental and numerical results are probably caused by differences between the actual and assumed nozzle exit conditions.[67]

The MOC simulation of flows with vibrational nonequilibrium may be partially verified by comparing the results with those obtained under the assumptions of vibrational freezing and full equilibrium. These cases bound the expected results and should reproduce them, in the appropriate limits. Consider an axisymmetric freejet composed of 95% N_2 and 5% NO (with $\Theta_{vib} = 3350$ and 2700 K, respectively), issuing from a reservoir with $P_s = 3$ atm and $T_s = 3000$ K, through a converging nozzle with $D = 5$ mm, into an ambient region with $P_a = 0.03$ atm. The flow has been simulated by the MOC with $M_i = 1.01$, $N_i \approx 25$, and $0.7 < \beta < 0.8$ deg. VET rates ranging from the base values obtained from the literature[3,34,57] to values 10^3 times as high are used, although, in each case, vibrational equilibrium is assumed to exist upstream of the nozzle exit, to simplify interpretation of the results. A version of the MOC procedure developed for vibrationally equilibrated flows has been used to simulate a freejet with identical nozzle exit conditions, by the use of an IV line with $M_i = 1.0496$, rather than 1.01, required because of the difference in the sound speeds calculated under frozen and equilibrated conditions.[3] An MOC computation for a freejet with $\gamma = \frac{7}{5}$, $P_s = 2.965$ atm, and $T_s = 3106$ K has also been performed, using the characteristic and compatibility equations appropriate for vibrationally frozen flows.[3] The small changes in the stagnation properties from those used in the other simulations are necessary to create equivalent conditions at the nozzle exit.

Figure 7a illustrates the slight variations in the locations of the primary jet features caused by changes in the model used for the vibrational state of the gas; Fig. 7b shows the predictions of the translation–rotational temperature, i.e., T, and the vibrational temperatures for N_2 and NO, i.e., T_{vib,N_2} and $T_{vib,NO}$, respectively, as functions of normalized distance along the jet axis. These results verify that the flow equations are correctly implemented in the MOC computation with vibrational nonequilibrium, insofar as its results

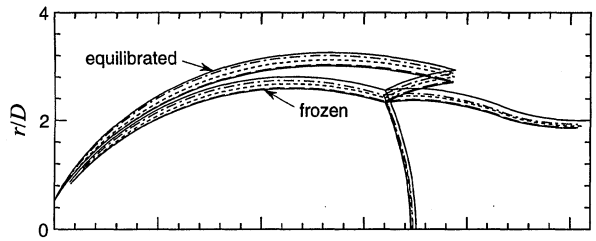

a) Primary features

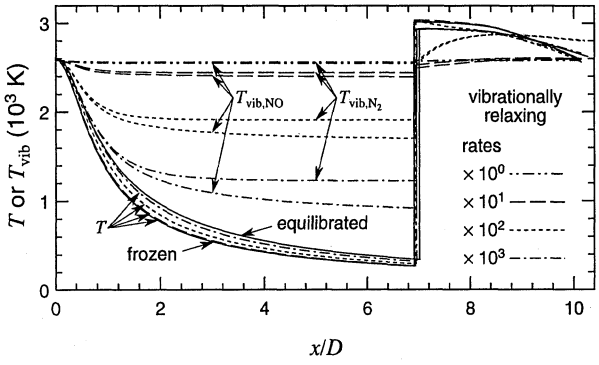

b) Axial profiles of translational–rotational and vibrational temperatures

Fig. 7 MOC results for freejets of 95% N_2 and 5% NO with $P_s/P_a \approx$ 100 under vibrationally frozen, relaxing, and equilibrated conditions.

fall between those obtained for frozen and equilibrated flows, in a logical order, according to the magnitude of the VET rates.

The general trends for T_{vib,N_2} and $T_{vib,NO}$ seen in Fig. 7b also follow those observed experimentally in a nozzle flow[68] and are consistent with the behavior anticipated from studies of VET behind planar shock waves.[57] Specifically, the vibrational state of the gas is expected to relax most efficiently in the high-pressure regions of the flow, near the nozzle exit and in the subsonic core. As the gas travels through the primary expansion, the rapid declines in pressure and temperature cause a near cessation of VET and the vibrational energies freeze. Strong V–V coupling, present because of the relatively small difference between Θ_{vib,N_2} and $\Theta_{vib,NO}$, governs the relaxation process, effectively increasing the rate at which N_2 relaxes and slowing the rate of NO relaxation. Final values of T_{vib,N_2} and $T_{vib,NO}$ in the expansion that are lower and higher, respectively, than they would be in the absence of V–V energy transfer result. However, as the coupling is incomplete, i.e., $\tau^{V-V}_{N_2-NO}$ is finite, the final, frozen values of T_{vib,N_2} and $T_{vib,NO}$ differ by an amount dependent on the degree of relaxation toward equilibrium with the translational–rotational modes of the gas. $T_{vib,NO}$ is consistently closer to T than T_{vib,N_2} is, because the self-relaxation rate for NO is orders of magnitude higher than that for N_2.

An increase in the scale of the flow, i.e., D, or in its overall pressure, i.e., P_s and P_a, has an effect identical to a proportional increase in the VET rates. However, for given VET rates and fixed values of D and P_s, an increase in the mole fraction of NO magnifies the effect of V–V coupling, making the relative differences between T_{vib,N_2} and $T_{vib,NO}$ smaller, as well as increasing the overall relaxation rate of the gas.

Conclusion

In this work, the partial-differential equations describing the steady, two-dimensional flow of a perfect gas undergoing vibrational relaxation were transformed to ODEs applicable on characteristic coordinates, thereby permitting the relatively simple computational solution of several supersonic flow problems. The MOC was implemented numerically to simulate a highly underexpanded freejet flow with vibrational nonequilibrium, in addition to being applied to freejets of gases with complete vibrational freezing or equilibrium. In regions of the flow where the smallest effective VET time constant was comparable to the temporal-step size, i.e., (spatial-step size)/velocity, in a steady flow, an explicit method of integration with second-order accuracy was used for the equations of motion and an implicit method with first-order accuracy was used for the equations describing vibrational relaxation. Elsewhere in the vibrationally nonequilibrated flow simulation and in the entire calculation of the flow of a vibrationally frozen or equilibrated gas, the equations were integrated by a fully second-order-accurate, explicit method.

A comparison of the MOC results with a correlation for the flow properties along the axis of an axisymmetric jet demonstrated that the computational techniques were valid for vibrationally frozen flows and indicated the maximum angular spacing of the characteristics launched from the nozzle lip required to maintain the accuracy of the solution downstream, where the grid resolution fell due to the spreading of the Mach lines with increasing flow speed. Empirically based correlations giving the length of the barrel-shock structure as a function of pressure ratio were compared with the results of the MOC simulation and found to be in excellent agreement with them. Good agreement was also observed between the MOC predictions and experimental data for the radius of the Mach disk, although discrepancies likely attributable to inaccuracies in the shape of the IV line remained.

Results from MOC simulations of a freejet under vibrationally frozen, relaxing, and equilibrated conditions were compared to verify the approach used for flows with active vibrational relaxation. It was shown that, in the appropriate limits, the results agreed with those obtained for vibrationally frozen and equilibrated gases. Although these findings are encouraging, full validation of the simulation technique for two-dimensional flows would require comparisons with experimental data that are beyond the scope of the present discussion and that, to a large extent, would depend on the accuracy of the VET rates used. However, the simulation techniques demonstrated here provide a laboratory tool useful for examining the effects of vibrational relaxation and for planning and predicting the results of experiments conducted in freejet flows.

Acknowledgments

This work was supported under a Contract from the Air Force Office of Scientific Research with Julian Tishkoff as Technical Monitor.

References

[1]Zucrow, M. J., and Hoffman, J. D., *Gas Dynamics*, Vol. 1, Wiley, New York, 1976, Chap. 12.

[2]Zucrow, M. J., and Hoffman, J. D., *Gas Dynamics—Multidimensional Flow*, Vol. 2, Krieger, Malabar, FL, 1986, Chaps. 16–18.

[3]Palmer, J. L., "Temporally Resolved Velocimetry in a Shock-Tunnel Free Jet by Planar Fluorescence Imaging of Nitric Oxide," Ph.D. Thesis, Dept. of Mechanical Engineering, Stanford Univ., Stanford, CA, June 1997.

[4]Pack, D. C., "On the Formation of Shock-Waves in Supersonic Gas Jets (Two-Dimensional Flow)," *Quarterly Journal of Mechanics and Applied Mathematics*, Vol. 1, Pt. 1, 1948, pp. 1–17.

[5]Vick, A. R., Andrews, E. H., Dennard, J. S., and Craidon, C. B., "Comparisons of Experimental Free-Jet Boundaries with Theoretical Results Obtained with the Method of Characteristics," NASA TN D-2327, June 1964.

[6]Volkonskaya, T. G., "Calculation of Supersonic Axisymmetric Jets," *Numerical Methods in Gas Dynamics*, edited by G. S. Roslyakov and L. A. Chudov, Vol. 2, Collection of Papers of the Computational Center of the Moscow State Univ., Translated from Russian, Israel Program for Scientific Translation, Jerusalem, Israel, 1966, pp. 51–56.

[7]Sheeran, W. J., and Dosanjh, D. S., "Observations on Jet Flows from a Two-Dimensional, Underexpanded, Sonic Nozzle," *AIAA Journal*, Vol. 6, No. 3, 1968, pp. 540–542.

[8]Goffe, D., "Modélisation numérique par la méthod des caractéristiques, et etude experiméntale de jets supersonique libres," Thése de Docteur Ingénieur, Ecole Centrale des Arts et Manufactures, Chatenay-Malabry, France, Oct. 1984.

[9]Eastman, D. W., and Radtke, L. P., "Location of the Normal Shock Wave in the Exhaust Plume of a Jet," *AIAA Journal*, Vol. 1, No. 4, 1963, pp. 918, 919.

[10]Peters, C. E., and Phares, W. J., "The Structure of Plumes from Moderately Underexpanded Supersonic Nozzles," AIAA Paper 70-229, Jan. 1970.

[11]Abbett, M., "The Mach Disk in Underexpanded Exhaust Plumes," *AIAA Journal*, Vol. 9, No. 3, 1970, pp. 512–514.

[12]Fox, J. H., "On the Structure of Jet Plumes," *AIAA Journal*, Vol. 12, No. 1, 1974, pp. 105–107.

[13]Salas, M. D., "The Numerical Calculation of Inviscid Plume Flowfields," AIAA Paper 74-523, June 1974.

[14]Dash, S. M., and Thorpe, R. D., "Shock-Capturing Model for One- and Two-Phase Supersonic Exhaust Flow," *AIAA Journal*, Vol. 19, No. 7, 1981, pp. 842–851.

[15]Norman, M. L., Smarr, L., Winkler, K.-H. A., and Smith, M. D., "Structure and Dynamics of Supersonic Jets," *Astronomy and Astrophysics*, Vol. 113, No. 2, 1982, pp. 285–302.

[16]Gottlieb, J. J., and Shi, Z. C., "Random-Choice-Method Solutions for Two-Dimensional Planar and Axisymmetric Steady Supersonic Flows," *Israel Journal of Technology*, Vol. 23, No. 4, 1986/7, pp. 153–168.

[17]Palacio, A., Malin, M. R., Proumen, N., and Sanchez, L., "Numerical Computations of Steady Transonic and Supersonic Flow Fields," *International Journal of Heat and Mass Transfer*, Vol. 33, No. 6, 1990, pp. 1193–1204.

[18]Kim, C. M., Krejsa, E. A., and Khavaran, A., "Significance of Shock Structure on Supersonic Jet Mixing Noise of Axisymmetric Nozzles," *AIAA Journal*, Vol. 32, No. 9, 1994, pp. 1920–1923.

[19]Nishida, M., Nomura, H., and Aso, S., "Numerical Simulation of Shock Waves Generated by an Opposing Jet," *Shock Waves—Proceedings of the 18th International Symposium on Shock Waves*, edited by K. Takayama, Vol. 2, Springer–Verlag, Berlin, 1992, pp. 1081–1086.

[20]Capiaux, R., and Washington, M., "Nonequilibrium Flow Past a Wedge," *AIAA Journal*, Vol. 1, No. 3, 1963, pp. 650–660.

[21]Sedney, R., and Gerber, N., "Nonequilibrium Flow over a Cone," *AIAA Journal*, Vol. 1, No. 11, 1963, pp. 2482–2486.

[22]Wood, A. D., Springfield, J. F., and Pallone, A. J., "Chemical and Vibrational Relaxation of an Inviscid Hypersonic Flow," *AIAA Journal*, Vol. 2, No. 10, 1964, pp. 1697–1705.

[23]Gzhelyak, R. A., and Dubinskaya, N. V., "Application of the MOC to Calculations of Nonequilibrium Supersonic Air Flow Past Blunted Cones," NASA TT F-11 691, May 1968.

[24]Appleton, J. P., "Structure of a Prandtl–Meyer Expansion in an Ideal Dissociating Gas," *Physics of Fluids*, Vol. 6, No. 8, 1963, pp. 1057–1062.

[25]Glass, I. I., and Takano, A., "Nonequilibrium Expansion Flows of Dissociated Oxygen and Ionized Argon Around a Corner," *Progress in Aeronautical Sciences*, edited by D. Küchemann and L. H. G. Sterne, Vol. 6, Pergamon, Oxford, England, UK, 1965, pp. 163–249.

[26]Der, J. J., "Theoretical Studies of Supersonic Two-Dimensional and Axisymmetric Nonequilibrium Flow, Including Calculations of Flow Through a Nozzle," NASA TR R-164, Dec.1963.

[27]Rizkalla, O., Chinitz, W., and Erdos, J. I., "Calculated Chemical and Vibrational Nonequilibrium Effects in Hypersonic Nozzles," *Journal of Propulsion and Power*, Vol. 6, No. 1, 1990, pp. 50–57.

[28]Quan, V., Melde, J. E., Kleigel, J. R., Nickerson, G. R., and Frey, H. M., "Kinetic Performance of Barrier-Cooled Rocket Nozzles," *Journal of Spacecraft and Rockets*, Vol. 5, No. 10, 1968, pp. 1137–1142.

[29]Quan, V., "Analytical Predictions of Delivered Specific Impulse," NASA CR-1123, Aug. 1969.

[30]Sedney, R., "The Method of Characteristics," *Nonequilibrium Flows*, Pt. 2, edited by P. P. Wegner, Marcel Dekker, New York, 1970, pp. 159–225.

[31]Johnson, G. R., "Supersonic Gas–Solid Particle Flow in an Axisymmetric Nozzle by the Method of Characteristics," von Kármán Inst. for Fluid Dynamics, TN 78, Rhode-Saint-Gênese, Belgium, Aug. 1971.

[32]Ishii, R., and Umeda, Y., "Free-Jet Flows of Gas-Particle Mixtures," *Journal of Thermophysics and Heat Transfer*, Vol. 2, No. 1, 1988, pp. 17–24.

[33]Quan, V., and Kleigel, J. R., "Axisymmetric Two-Phase Reacting Gas Nonequilibrium Nozzle Flows Analysis," TRW Systems, Rept. 02874-6007-R000, Redondo Beach, CA, Aug. 1967.

[34]Millikan, R. C., and White, D. R., "Systematics of Vibrational Relaxation," *Journal of Chemical Physics*, Vol. 39, No. 12, 1963, pp. 3209–3213.

[35]Vincenti, W. G., and Kruger, C. H., *Introduction to Physical Gas Dynamics*, Krieger, Malabar, FL, 1965, Chap. 7.

[36]Blackman, V., "Vibrational Relaxation in Oxygen and Nitrogen," *Journal of Fluid Mechanics*, Vol. 1, Pt. 1, 1956, pp. 61–85.

[37]Appleton, J. P., "Shock-Tube Study of the Vibrational Relaxation of Nitrogen Using Vacuum-Ultraviolet Light Absorption," *Journal of Chemical Physics*, Vol. 47, No. 9, 1967, pp. 3231–3240.

[38]Hanson, R. K., and Baganoff, D., "Shock-Tube Study of Vibrational Relaxation in Nitrogen Using Pressure Measurements," *Journal of Chemical Physics*, Vol. 53, No. 11, 1970, pp. 4401–4403.

[39]Hurle, I. R., Russo, A. L., and Hall, J. G., "Spectroscopic Studies of Vibrational Nonequilibrium in Supersonic Nozzle Flows," *Journal of Chemical Physics*, Vol. 40, No. 8, 1964, pp. 2076–2089.

[40]Hurle, I. R., and Russo, A. L., "Spectrum-Line Reversal Measurements of Free-Electron and Coupled N_2 Vibrational Temperatures in Expansion Flows," *Journal of Chemical Physics*, Vol. 43, No. 12, 1965, pp. 4434–4443.

[41]Sebacher, D. I., "An Electron Beam Study of Vibrational and Rotational Relaxing Flows of Nitrogen and Air," *Proceedings of the 1966 Heat Transfer and Fluid Mechanics Institute*, edited by M. A. Saad and J. A. Miller, Stanford Univ. Press, Stanford, CA, 1966, pp. 315–334.

[42]Von Rosenberg, C. W., Taylor, R. L., and Teare, J. D., "Vibrational Relaxation of CO in Nonequilibrium Nozzle flow," *Journal of Chemical Physics*, Vol. 48, No. 12, 1968, pp. 5731–5733.

[43]Hurle, I. R., "Nonequilibrium Flows with Special Reference to the Nozzle-Flow Problem," *Shock Tube Research—Proceedings of the 8th International Shock Tube Symposium*, edited by J. L. Stollery, A. G. Gaydon, and P. R. Owen, Chapman and Hall, London, 1971, pp. 3/1–3/37.

[44]Hsu, C. F., and Maillie, F. H., "Vibrational Relaxation of Anharmonic Oscillators with Vibration–Vibration and Vibration–Translation Energy Exchanges," *Journal of Chemical Physics*, Vol. 52, No. 4, 1970, pp. 1767–1772.

[45]Sharma, S. P., Ruffin, S. M., Gillespie, W. D., and Meyer, S. A., "Nonequilibrium Vibrational Population Measurements in an Expanding Flow Using Spontaneous Raman Spectroscopy," AIAA Paper 92-2855, July 1992.

[46]Gillespie, W. D., Bershader, D., Sharma, S. P., and Ruffin, S. M., "Raman Scattering Measurements of Vibrational and Rotational Distributions in Expanding Nitrogen," AIAA Paper 93-0274, Jan. 1993.

[47]Rich, J. W., and Rehm, R. G., "Population Distributions During Vibrational Relaxation of Diatomic Gases," *Proceedings of the Eleventh Symposium (International) on Combustion*, Combustion Inst., Pittsburgh, PA, 1967, pp. 37–48.

[48]Bray, K. N. C., "Vibrational Relaxation of Anharmonic Oscillator Molecules: Relaxation Under Isothermal Conditions," *Journal of Physics B, Proceedings of the Physical Society (Atomic and Molecular Physics)*, Ser. 2, Vol. 1, No. 4, 1968, pp. 705–717.

[49]McKenzie, R. L., "Diatomic Gasdynamic Lasers," *Physics of Fluids*, Vol. 15, No. 12, 1972, pp. 2163–2173.

[50]Bender, D. J., Mitchner, M., and Kruger, C. H., "Measurement of Vibrational Population Distributions in a Supersonic Expansion of Carbon Monoxide," *Physics of Fluids*, Vol. 21, No. 7, 1978, pp. 1073–1085.

[51]Center, R. E., and Caledonia, G. E., "Anharmonic Effects in the Vibrational Relaxation of Diatomic Molecules in Expanding Flows," *Applied Optics*, Vol. 10, No. 8, 1971, pp. 1795–1802.

[52]Chiroux de Gavelle de Roany, A., Flament, C., Rich, J. W., Subramanian, V. V., and Warren, W. R., "Strong Vibrational Nonequilibrium in Supersonic Nozzle Flows," *AIAA Journal*, Vol. 31, No. 1, 1993, pp. 119–128.

[53]Ruffin, S. M., and Park, C., "Vibrational Relaxation of Anharmonic Oscillators in Expanding Flows," *Journal of Spacecraft and Rockets*, Vol. 30, No. 1, 1993, pp. 59–68.

[54]Blom, A. P., Bray, K. N. C., and Pratt, N. H., "Rapid Vibrational De-Excitation Influenced by Gasdynamic Coupling," *Astronautica Acta*, Vol. 15, Nos. 5/6, 1970, pp. 487–493.

[55]Canupp, P. W., Candler, G. V., Perkins, J. N., and Erickson, W. D., "Analysis of Hypersonic Nozzles Including Vibrational Nonequilibrium and Intermolecular Force Effects," *AIAA Journal*, Vol. 31, No. 7, 1993, pp. 1243–1249.

[56]Park, C., and Lee, S.-H., "Validation of Multitemperature Nozzle Flow Code," *Journal of Thermophysics and Heat Transfer*, Vol. 9, No. 1, 1995, pp. 9–16.

[57]Taylor, R. L., Camac, M., and Feinberg, R. M., "Measurements of Vibration–Vibration Coupling in Gas Mixtures," *Eleventh Symposium (International) on Combustion*, Combustion Inst., Pittsburgh, PA, 1967, pp. 49–65.

[58]Cottrell, T. L., and McCoubrey, J. C., *Molecular Energy Transfer in Gases*, Butterworths, London, 1961, pp. 27–29.

[59]Kung, R. T. V., and Center, R. E., "High Temperature Vibrational Relaxation of H_2O by H_2O, He, Ar, and N_2," *Journal of Chemical Physics*, Vol. 62, No. 6, 1975, pp. 2187–2194.

[60]Tyson, T. J., "An Implicit Integration Method for Chemical Kinetics," TRW Space Technology Lab., Rept. 9840-6002-RU000, Redondo Beach, CA, Sept. 1964.

[61]Press, W. H., Flannery, B. P., Teukolsky, S. A., and Vetterling, W. T., *Numerical Recipes—The Art of Scientific Computing*, Cambridge Univ. Press, New York, 1986, p. 272.

[62]Kleigel, J. R., and Quan, V., "Convergent–Divergent Nozzle Flows," *AIAA Journal*, Vol. 6, No. 9, 1968, pp. 1728–1734.

[63]Ashkenas, H., and Sherman, F. S., "The Structure and Utilization of Supersonic Free Jets in Low Density Wind Tunnels," *Advances in Applied Mechanics—Rarefied Gas Dynamics*, edited by J. H. de Leeuw, Vol. 2, Academic, New York, 1966, pp. 84–105.

[64]Crist, S., Sherman, P. M., and Glass, D. R., "Study of Highly Underexpanded Sonic Jet," *AIAA Journal*, Vol. 4, No. 1, 1968, pp. 68–71.

[65]Lewis, C. H., and Carlson, D. J., "Normal Shock Location in Underexpanded Gas and Gas-Particle Jets," *AIAA Journal*, Vol. 2, No. 4, 1964, pp. 776, 777.

[66]Love, E. S., Grigsby, C. E., Lee, L. P., and Woodling, M. J., "Experimental and Theoretical Studies of Axisymmetric Free Jets," NASA TR R-6, 1959.

[67]Campbell, D. H., "Direct Simulation Monte Carlo Analysis of the Near Field of Free Jets," AIAA Paper 89-1714, June 1989.

[68]Babikian, D. S., Gopaul, N. K. J. M., and Park, C., "Measurement and Analysis of Nitric Oxide Radiation in an Arc-Jet Flow," AIAA Paper 93-2800, July 1993.

K. Kailasanath
Associate Editor